2 May 2025

Modeling CO2 Adsorption in Flexible MOFs with Open Metal Sites via Fragment-Based Neural Network Potentials

Omer Tayfuroglu[1], Seda Keskin[1]

1. Koç University

Abstract

Metal-organic frameworks (MOFs) with open metal sites (OMS) are among the most promising porous materials for gas adsorption and separation, owing to their strong and selective interactions with guest molecules. However, simulating adsorption in such systems with high accuracy and efficiency remains a key challenge due to the need to model complex guest–MOF interactions and framework flexibility. Classical force fields often lack the precision to capture these effects, while ab initio methods are computationally prohibitive for large-scale, long-timescale simulations. In this work, we develop a neural network potential (NNP) trained on highly accurate DFT (PBE-D4/def2-TZVP) level data derived from a single representative fragment of the Mg-MOF-74 framework, a prototypical OMS-containing MOF, with CO2 molecules. Despite the limited training domain, the NNP accurately captured both intra- and intermolecular interactions in the CO2–Mg-MOF-74 system, including those involving the open metal sites. We integrated this NNP into a hybrid molecular dynamic (MD) and grand canonical Monte Carlo (GCMC) simulation workflow, enabling accurate modeling of CO2 adsorption in flexible MOFs. This approach allows us accounting for both framework dynamics and complex host–guest interactions with chemical accuracy and computational efficiency. Our results highlight the crucial role of framework flexibility in adsorption behavior and demonstrate that fragment-based NNP, when combined with advanced simulation techniques, offer a powerful and efficient approach for realistically modeling adsorption processes in MOFs with open metal sites.

Posted on 2 May 2025 — CC-BY-NC-ND 4.0 — This is a preprint and has not been peer reviewed. Data may be preliminary. — https://doi.org/10.26434/chemrxiv-2025-c85xt

Modeling CO_2 Adsorption in Flexible MOFs with Open Metal Sites via Fragment-Based Neural Network Potentials

Omer Tayfuroglu[1], Seda Keskin[2]

Department of Chemical and Biological Engineering, Koc University, Rumelifeneri Yolu, Sariyer, 34450 Istanbul, Turkey

Abstract

Metal-organic frameworks (MOFs) with open metal sites (OMS) are among the most promising porous materials for gas adsorption and separation, owing to their strong and selective interactions with guest molecules. However, simulating adsorption in such systems with high accuracy and efficiency remains a key challenge due to the need to model complex guest–MOF interactions and framework flexibility. Classical force fields often lack the precision to capture these effects, while ab initio methods are computationally prohibitive for large-scale, long-timescale simulations. In this work, we develop a neural network potential (NNP) trained on highly accurate DFT (PBE-D4/def2-TZVP) level data derived from a single representative fragment of the Mg-MOF-74 framework, a prototypical OMS-containing MOF, with CO_2 molecules. Despite the limited training domain, the NNP accurately captured both intra- and intermolecular interactions in the CO_2–Mg-MOF-74 system, including those involving the open metal sites. We integrated this NNP into a hybrid molecular dynamic (MD) and grand canonical Monte Carlo (GCMC) simulation workflow, enabling accurate modeling of CO_2 adsorption in flexible MOFs. This approach allows us accounting for both framework dynamics and complex host–guest interactions with chemical accuracy and computational efficiency. Our results highlight the crucial role of framework flexibility in adsorption behavior and demonstrate that fragment-based NNP, when combined with advanced simulation techniques, offer a powerful and efficient approach for realistically modeling adsorption processes in MOFs with open metal sites.

Keywords: MOFs, OMS, machine learning potentials, DFT, flexible framework.

[1]Corresponding Author: Omer Tayfuroglu, Department of Chemical and Biological Engineering, Koc University, otayfuroglu@ku.edu.tr, +90 (212) 338-1362

[2] Corresponding Author: Seda Keskin, Department of Chemical and Biological Engineering, Koc University, skeskin@ku.edu.tr, +90 (212) 338-1362

https://doi.org/10.26434/chemrxiv-2025-c85xt **ORCID:** https://orcid.org/0000-0001-7834-3132 Content not peer-reviewed by ChemRxiv. **License:** CC BY-NC-ND 4.0

1. Introduction:

Metal-organic frameworks (MOFs) have emerged as a versatile class of porous materials, drawing considerable attention thanks to their potential in a wide range of applications such as gas adsorption, storage [1–5] and separation [6–9], drug delivery [10–13], chemical sensing [14] and catalysis [15,16]. Their modular architecture, with numerous combinations of metal nodes and organic linkers, allows a wide range of remarkable functionalities by fine-tuning their structural and chemical properties. Among many types of MOFs, a notable subclass is MOFs having open metal sites (OMS) which serve as strong binding centers for the guest molecules. These coordinatively unsaturated metal centers significantly enhance interactions with the adsorbate molecules, making OMS-containing MOFs particularly effective in catalysis [17] and selective gas adsorption [18,19].

One representative example is Mg-MOF-74 (also known as Mg_2(dobpdc) and Mg-CPO-27), a benchmark MOF whose channels are decorated with accessible Mg sites [20,21]. This structure has exceptional performance in the selective capture of CO_2, even in the presence of other gases such as H_2, CH_4, and H_2O, making it a model system for studying molecule-specific adsorption in MOFs [17,21–23]. Mg-MOF-74 has been extensively studied for the adsorption of various gas molecules, including CO_2, N_2, CO, C_2H_2 and CH_4, and demonstrated significant advantages in the separation of light hydrocarbon mixtures [24–28]. These examples highlight the crucial role that OMS play in adsorption-related applications of MOFs and underscore the need for a deeper understanding of OMS–guest molecule interactions to guide the design of novel MOFs with enhanced performance. Gaining atomistic-level insight into these interactions often lies beyond the reach of current experimental techniques. Molecular simulations offer a powerful complement by providing detailed atomistic insights and aiding in the interpretation and guidance of experimental studies. From a computational perspective, accurate modeling of guest–MOF systems is essential for reliably predicting adsorption behavior and performance, ultimately guiding the rational design of advanced adsorbent materials. As recently demonstrated by Goeminne et al. [29], two major challenges remain in effectively simulating these complex host–guest systems: First, a reliable and accurate force field is required to accurately represent the potential energy surface (PES). Second, accurate modeling of the adsorption dynamics of the host–guest system is crucial for sufficient sampling of the PES.

https://doi.org/10.26434/chemrxiv-2025-c85xt **ORCID:** https://orcid.org/0000-0001-7834-3132 Content not peer-reviewed by ChemRxiv. **License:** CC BY-NC-ND 4.0

The first challenge concerns the method used to compute the PES, which captures both intra- and intermolecular interactions. Achieving an accurate adsorption isotherm requires methods capable of determining intermolecular interactions between guest molecules and the host framework with a high chemical accuracy. However, the large number of iterations required for the convergence of Monte Carlo simulations often necessitates the use of computationally inexpensive force fields. In this context, classical force field (FF)-based simulations offer a practical compromise, and they have been widely applied to study both the adsorption and diffusion of guest molecules in MOFs [30–33]. Most theoretical studies rely on Lorentz–Berthelot mixing rules to combine generic force fields (e.g., universal force field (UFF), Dreiding) for MOFs with various guest models [34,35]. While this simplified approach performs reasonably well for small molecules in coordinatively saturated MOFs, it becomes inadequate for systems with more complex interactions. For instance, force fields like TraPPE [36] effectively model CO_2–CO_2 interactions, but their combination with generic MOF force fields for CO_2–MOF interactions can reduce the overall simulation accuracy [37].

Accurate modeling of guest–OMS interactions necessitate the specialized force field parameterization, which remains a complex and non-trivial task [38]. This emphasizes the need for advanced force fields that combine chemical accuracy with computational efficiency to capture the full range of interactions in these systems. First-principles quantum mechanical methods, such as density functional theory (DFT), offer a precise way to characterize these complex interactions, especially those involving open metal sites. Thus, researchers have increasingly turned to quantum mechanical approaches to study the gas adsorption in MOFs. To explicitly investigate CO_2 adsorption in Mg-MOF-74 with ab initio accuracy, several strategies have been employed. For example, Kundu et al. used well-defined adsorption sites and conducted grand canonical Monte Carlo (GCMC) simulations with interaction energies calculated at a correlated wave function-corrected DFT-level to predict the CO_2 adsorption isotherms [39,40]. More recently, Fetisov et al. and Goeminne et al. eliminated the need for predefined adsorption sites by directly performing GCMC simulations on DFT-derived PES [39–41]. Despite the high accuracy of ab initio methods, their applications to guest–MOF systems remain computationally demanding, especially considering the large unit cells that often contain thousands of atoms [42,43]. Reliable modeling of processes such as adsorption and diffusion requires extensive sampling and long simulation times to capture the dynamic nature of these interactions. However, the computational cost of first-

https://doi.org/10.26434/chemrxiv-2025-c85xt **ORCID:** https://orcid.org/0000-0001-7834-3132 Content not peer-reviewed by ChemRxiv. **License:** CC BY-NC-ND 4.0

principles simulations typically limits their applicability to systems with fewer than a few hundred atoms and time scales restricted to the picosecond regime, as in ab initio molecular dynamics (AIMD) [44]. These limitations make it extremely challenging to investigate guest adsorption in MOFs over the long timescales and large length scales relevant to experimental conditions.

To overcome the limitations of both classical force fields and ab initio methods, a compromise between accuracy and computational efficiency is offered by machine learning potentials (MLPs). These models are trained on reference data generated from DFT calculations and they can accurately reproduce the underlying PES at a fraction of the computational cost. As such, MLPs present a compelling alternative to conventional force fields, with the potential to capture the complex interactions in MOFs having OMS while enabling simulations at larger length and time scales. Following the pioneering work by Behler and colleagues [45], who developed neural network potentials (NNPs) using a high-dimensional neural network (HDNN) architecture for isoreticular MOFs, numerous MLPs have been introduced for both MOF structures and guest–MOF systems [29,46–51].

The second challenge concerns the development of a reliable method for sampling the PES of guest–MOF systems. In this context, two key aspects must be addressed: the computational efficiency of modeling guest adsorption through GCMC simulations, and the inclusion of framework flexibility. Therefore, an integrated workflow is required to model the adsorption of guest molecules in flexible MOFs. To accurately model the dynamic behavior of MOFs and effectively capture their flexibility during guest adsorption, molecular dynamics (MD) simulations can be combined with GCMC simulations. This integrated approach enables the inclusion of both intrinsic and extrinsic flexibility—such as linker rotations, breathing, swelling, and structural contraction or expansion—triggered by thermal motion, gas adsorption, or mechanical stress. This methodology accounts for global structural changes (e.g., unit cell expansion or contraction) and reflects their impact on adsorption behavior [29]. Moreover, it also captures local structural flexibility, which can significantly influence the adsorption even in the absence of large-scale structural transitions, thereby improving the accuracy of simulation results.

Several efforts have been made to define effective simulation protocols that integrate classical force field-based GCMC and MD simulations [52,53]. For instance, Ghoufi and Maurin investigated the phase transitions of MIL-53, a flexible MOF, during CO_2 adsorption, capturing extrinsic flexibility using a combined MD/GCMC framework [54]. More recently, Sholl and co-

https://doi.org/10.26434/chemrxiv-2025-c85xt **ORCID:** https://orcid.org/0000-0001-7834-3132 Content not peer-reviewed by ChemRxiv. **License:** CC BY-NC-ND 4.0

workers employed a similar hybrid approach to screen MOFs using an adsorption relaxation model, which incorporates both extrinsic and intrinsic (adsorption-induced) flexibility [55]. In that work, UiO-66 appeared relatively insensitive to flexibility, though this may be a limitation of the classical force field used, as other studies suggest UiO-66 exhibits non-negligible flexibility. To address these limitations, Johnson and co-workers [56] employed a NNP trained on DFT data to model the diffusion of neon and xenon through UiO-66 using MD simulations. Their results demonstrated the superiority of NNPs over classical FFs in capturing accurate structural dynamics and showed the potential of hybrid approaches; using NNPs for the intra-molecular interaction of MOF and classical FFs for guest–guest interactions, combined through mixing rules for host–guest interactions. Tayfuroglu et al. [57] applied MD/GCMC simulations to flexible MOFs and found that structural relaxation significantly improved the agreement between simulated and experimental adsorption isotherms of H_2 and CH_4. Most recently, Zheng et al. [58] studied CO_2 adsorption in Mg-MOF-74, by systematically comparing its diffusivity in rigid and flexible frameworks using MD simulations based on MLPs. Their results demonstrated that incorporating flexibility with MLPs significantly influences diffusion behavior; however, the effect of framework flexibility on gas adsorption was not explored in their study.

As this literature review demonstrates, there is a strong need to develop MLPs to better understand both the guest–guest and guest–framework interactions in flexible MOF structures having OMS. Motivated from this, in this work, we developed an NNP trained on highly accurate DFT (PBE-D4/def2-TZVP) level data to model all relevant interactions in the CO_2–Mg-MOF-74 system, including guest–guest, guest–framework intermolecular interactions, and the intramolecular interactions within the MOF. Using this NNP, we implemented a hybrid MD/GCMC simulation method to study the adsorption dynamics of CO_2 in a flexible Mg-MOF-74 having OMS. This integrated approach allowed us to account for both structural flexibility and complex host–guest interactions, enabling a more realistic and chemically accurate description of the adsorption process in Mg-MOF-74.

2. Computational Strategy:

Figure 1 provides an overview of our computational approach to develop an NNP for the CO_2 adsorption in Mg-MOF-74, starting from fragments to accurately define all bonded and non-bonded interactions at the DFT (PBE-D4/def2-TZVP) level ending with the rigid/flexible GCMC

https://doi.org/10.26434/chemrxiv-2025-c85xt **ORCID:** https://orcid.org/0000-0001-7834-3132 Content not peer-reviewed by ChemRxiv. **License:** CC BY-NC-ND 4.0

simulations. Initially, a fragment was extracted from the bulk MOF structure, and the guest-host system was constructed. Next, an NNP was developed at the DFT level using an active learning approach. Finally, NNP-based rigid and flexible GCMC adsorption simulations were performed.

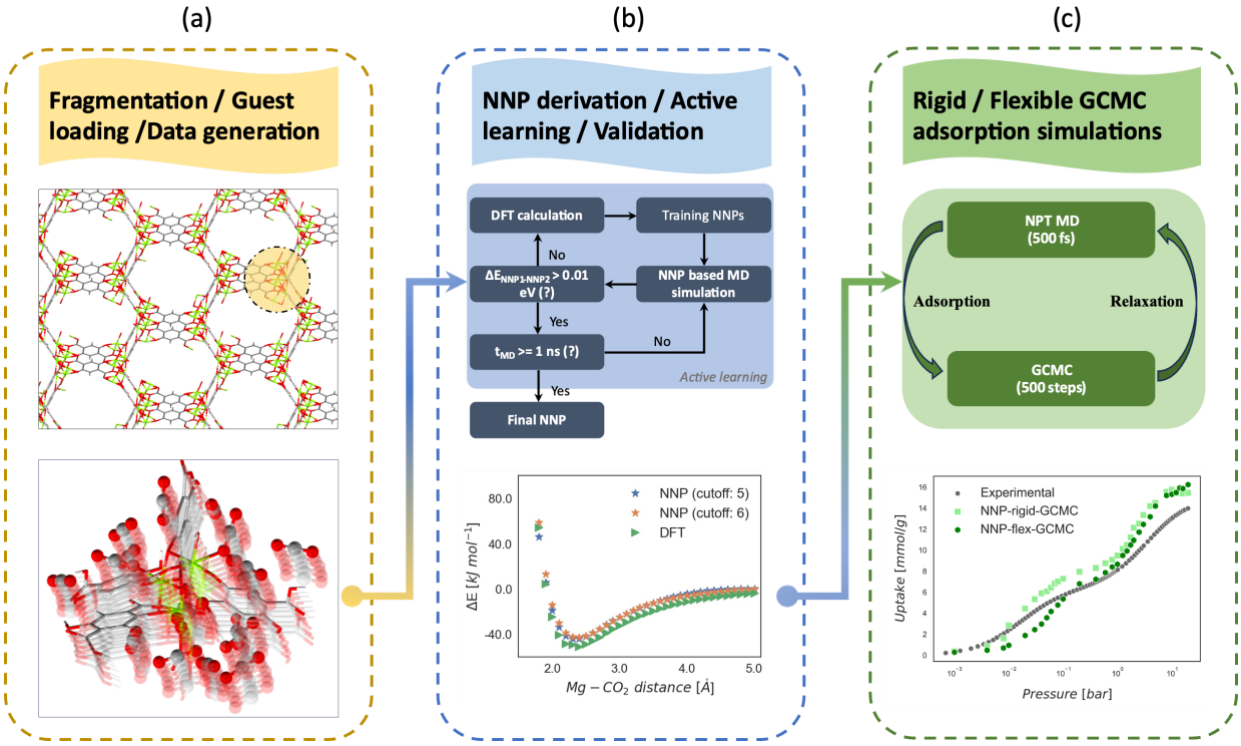


Figure 1. Workflow for the development of an NNP from a single fragment to its application in GCMC simulations. (a) Construction of the initial guest-host system. (b) Generation of the training dataset at the DFT-level and NNP development using an active learning scheme. (c) NNP-based rigid and flexible GCMC simulations to compute gas adsorption.

Training an NNP model requires computing the potential energy surface at DFT level, which can be computationally very expensive for the bulk MOF systems. To address this issue, we adopted a fragmentation approach which allows the efficient data generation while maintaining the accuracy [45,46]. Since the NNP models rely on atom centered features, the environment of atoms must be clearly defined within a certain cutoff. Thus, the MOF structure can be divided into the fragments by finding chemically inequivalent atoms that form the bulk structure. For the guest (CO_2)-loaded fragments, we employed the Neural Equivariant Interatomic Potentials (NequIP) to model PES, capturing both bonded and non-bonded interactions [59]. NequIP has been widely recognized for its success in modeling bonded interactions, demonstrating exceptional

https://doi.org/10.26434/chemrxiv-2025-c85xt **ORCID:** https://orcid.org/0000-0001-7834-3132 Content not peer-reviewed by ChemRxiv. **License:** CC BY-NC-ND 4.0

data efficiency and setting a benchmark in the field [59,60]. However, its performance is significantly affected when training on snapshots containing varying numbers of atoms, as the cost function in NequIP is sensitive to the system size. This issue becomes particularly relevant in guest-loaded fragments, where the number of atoms fluctuates. To mitigate this challenge, we trained our dataset using a single guest-loaded snapshot, ensuring consistency in the number of atoms across training samples.

As illustrated in **Figure 2**, we generated a fragment which includes all atom types and their neighbor atoms within a sphere of 6 Å cutoff radius. When extracting the fragment from Mg-MOF-74 [61], we avoided truncating phenyl rings and saturated missing bonds with hydrogen to maintain charge balance. The fragment was then placed in a simulation box and 32 CO_2 molecules were loaded into the fragment at 100 bar and 50 K to maximize CO_2–MOF and CO_2–CO_2 interactions. We completed the generation of our initial dataset by producing 300 random non-equilibrium geometries using the CO_2–MOF system with a Python script. While generating the equilibrium geometries, we ensured that the maximum displacement was not greater than 0.16 Å to prevent the formation of unphysical structures. Finally, DFT calculations were performed on these initial non-equilibrium geometries to generate energy and force data for constructing the initial training dataset. Using the NequIP, preliminary NNP models were then trained on this dataset to enable MD simulations for the active learning process.

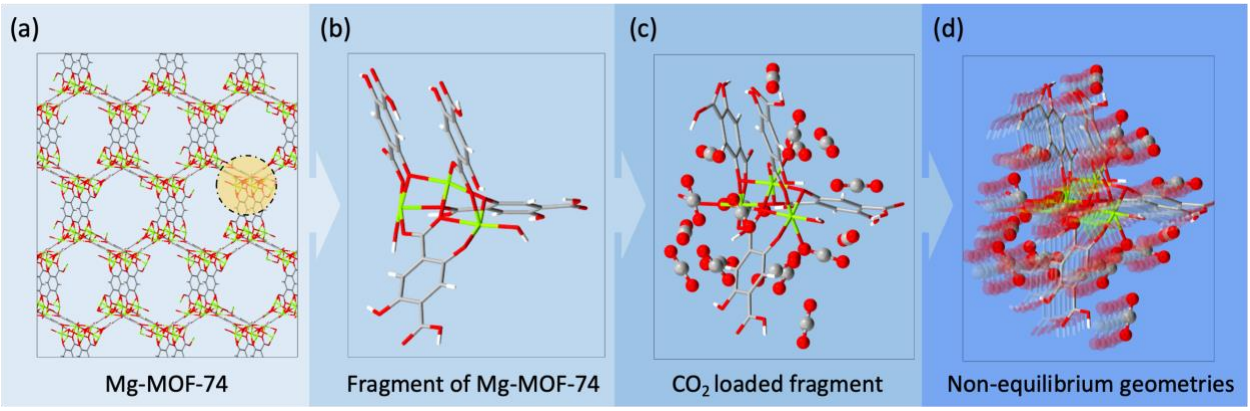


Figure 2. Preparation of the host-guest system: (a) bulk Mg-MOF-74, (b) extracted fragment, (c) CO_2 molecules added to the fragment, and (d) generation of random non-equilibrium geometries. The color code is as follows: green for Mg, red for O, gray for C, and white for H.

https://doi.org/10.26434/chemrxiv-2025-c85xt **ORCID:** https://orcid.org/0000-0001-7834-3132 Content not peer-reviewed by ChemRxiv. **License:** CC BY-NC-ND 4.0

Due to the initial dataset's limited ability to adequately represent the configuration space, incorporating missing structures from well-sampled regions is essential to enhance the dataset's comprehensiveness. Therefore, selecting and integrating new geometries into the training dataset must be done carefully. Here, our conformer selection process relies on an uncertainty-based criterion applied to structures obtained from NNP-driven MD simulations at different temperatures ranging from 50 to 500 K, carried out in the NVT ensemble. Specifically, for a given frame, we compared the energy predictions from two differently parameterized NNPs (NNP1 and NNP2), both trained on the same dataset but with different functional forms. If the energy difference between these two models (quantified as $\Delta E = E_{NNP1} - E_{NNP2}$) exceeded a predefined threshold for any configuration, that structure was considered critical for inclusion in the training set. Once enough new structures (approximately 300 data points) were identified through this procedure, these structures underwent DFT calculations, and they were subsequently added to the training dataset to refine the next generation of NNPs.

Using the trained NNP, we performed flexible GCMC simulations following the workflow illustrated in **Figure 3.** This method was implemented using a custom Python script that integrates the Atomic Simulation Environment (ASE) and LAMMPS software. As shown in **Figure 3(a),** this iterative process continues until the NNP reaches convergence, which was defined as the ability to perform stable and smooth NVT MD simulations for at least 1 ns without numerical instabilities or unphysical behaviors. At this point, the NNP was considered to adequately captured the relevant configuration space. To incorporate flexibility in the GCMC simulations, we employed a hybrid MD/GCMC method. This approach involves first the adsorption of gas molecules into the MOF using GCMC method, followed by MD simulations to relax the guest–MOF system. The sequential MD/GCMC simulations were performed using LAMMPS for MD and our in-house ASE-based GCMC code for the gas adsorption calculations. The workflow detailed in **Figure 3(b)** begins with energy minimization and thermal equilibration in the NVT ensemble. Subsequently, an NPT-MD simulation was initiated, during which GCMC operations (addition/removal and translation/rotation of gas molecules) were applied every 500 fs for 500 steps. Once gas adsorption within the MOF and structural and thermodynamic equilibrium were achieved (**Figure S1** and **S2** in the Supporting Information)-typically within this 1 ns duration- the simulation was terminated.

https://doi.org/10.26434/chemrxiv-2025-c85xt **ORCID:** https://orcid.org/0000-0001-7834-3132 Content not peer-reviewed by ChemRxiv. **License:** CC BY-NC-ND 4.0

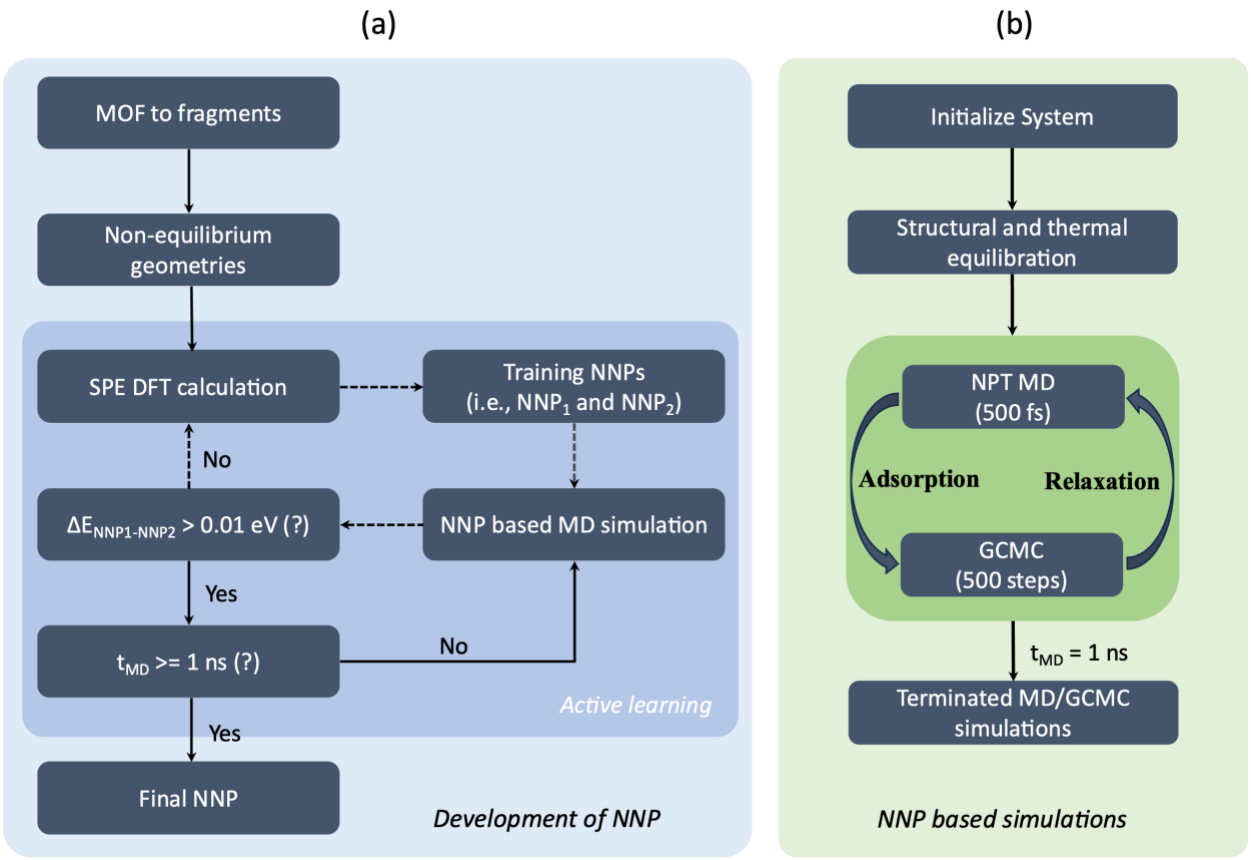


Figure 3. Algorithm flowcharts: (a) for the construction of NNP from MOF fragments with CO_2 based on DFT calculations and (b) flexible GCMC simulations.

3. Results and Discussions:

Using the active learning procedure outlined above, approximately 2000 conformers were obtained from a single fragment containing 32 molecules of CO_2 once the NNP was converged. To train the final NNP, the dataset was then divided into training (80%) and validation (20%) sets. The impact of various hyperparameters on both accuracy and computational efficiency was evaluated and optimal hyperparameters were determined as follows: a cutoff radius of 6 Å, 4 interaction layers, 32 features, and a maximum rotation order of 1. NequIP employs a loss function based on a weighted sum of energy and force loss terms [47,59], and we set these weighting factors to $\lambda_E = 10$ for energy and $\lambda_F = 1$. Early stopping was implemented when both the training and validation loss curves reached a plateau, defined as a change in validation loss of less than 0.005 eV over a patience period of 500 epochs (**Figure S3**).

https://doi.org/10.26434/chemrxiv-2025-c85xt **ORCID:** https://orcid.org/0000-0001-7834-3132 Content not peer-reviewed by ChemRxiv. **License:** CC BY-NC-ND 4.0

To evaluate the accuracy of the trained NNP on fragment, we generated approximately 200 non-equilibrium geometries from an NPT-MD simulation at 400 K, initiated from a randomly selected fragment. The NNP demonstrated excellent agreement with the results of DFT calculations, achieving R-squared values exceeding ~0.99 for both energy and atomic forces as shown in **Figure 4**. The RMSE values computed for the energy and forces also were 0.5 3 meV and 0.039 eV/atom, respectively.

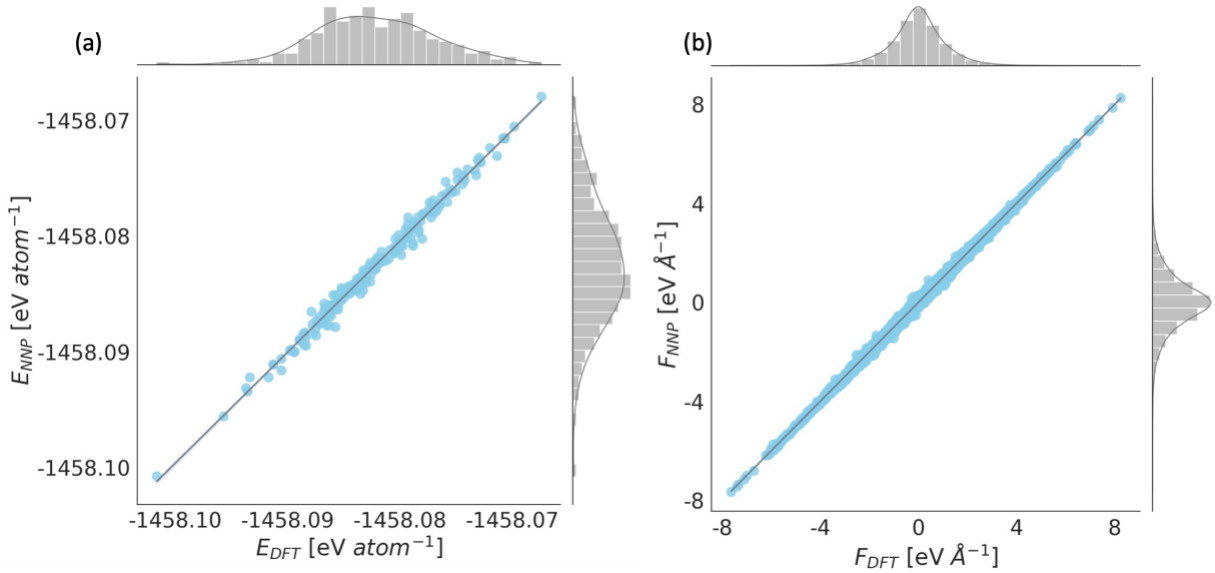


Figure 4. Comparison between the NNP predictions and DFT results for (a) energies and (b) forces for fragments.

Guest–MOF and guest–guest interactions play a crucial role in the GCMC simulations. At low pressures, guest–MOF interactions primarily govern the adsorption behavior, whereas at high pressures, guest–guest interactions become more significant. To assess the NNP's accuracy in capturing intermolecular interactions, we systematically scanned the distance between Mg–CO_2 and CO_2– CO_2 pairs from 1 to 6 Å in 0.2 Å increments. Then, for the obtained geometries, both NNP and reference DFT energies were calculated, and interaction energies were computed using the formula $E_{int} = E_{AB} - (E_A + E_B)$ where E_{AB} represents the total energy of the combined system, E_A and E_B correspond to the individual energies of the isolated components. For Mg–CO_2 interactions, A refers to the Mg center in the MOF fragment, and B represents a single CO_2 molecule. In the case of CO_2–CO_2 interactions, A and B both correspond to individual CO_2 molecules.

https://doi.org/10.26434/chemrxiv-2025-c85xt **ORCID:** https://orcid.org/0000-0001-7834-3132 Content not peer-reviewed by ChemRxiv. **License:** CC BY-NC-ND 4.0

Figure 5(a) shows that the NNP predictions for Mg–CO_2 interactions closely match the DFT reference values. At the equilibrium distance, the interaction energy is 44 kJ/mol for NNP and 52 kJ/mol for DFT, demonstrating good agreement with experimental values [22,24,62]. Similarly, the NNP accurately reproduces the DFT interaction energies for CO_2–CO_2 pairs, further validating its reliability in capturing intermolecular interactions as shown in **Figure 5(b)**. During hyperparameter optimization, we tested different cutoff values (details are given in the SI-Computational Methods section). Compared to the default 5 Å, training the NNP with a 6 Å cutoff significantly improved the accuracy of interaction energies beyond 3.5 Å, particularly for CO_2–CO_2 interactions. These long-range interactions are crucial in the GCMC simulations, where accurately modeling guest–guest interactions is essential for predicting adsorption behavior.

After validating the NNP on fragments, MD simulations, and intermolecular interaction energies, we further assessed its performance by computing the equilibrium bulk properties as a final test. To determine the NNP-based equilibrium lattice constants, we conducted NPT-MD simulations for 1 ns at 1 bar and 100 K, using the Nosé-Hoover thermostat and barostat. The last 0.5 ns of the simulations were analyzed to extract equilibrium bulk properties.

Table 1 compares the equilibrium lattice constants predicted by the NNP for the bulk Mg-MOF-74 with the experimentally reported single-crystal X-ray diffraction (SCXRD) values [25]. The NNP-predicted lattice constants exhibit excellent agreement with experiments, with deviations of only 0.04, 0.039, and 0.016 Å for the lattice constants of a, b, and c respectively.

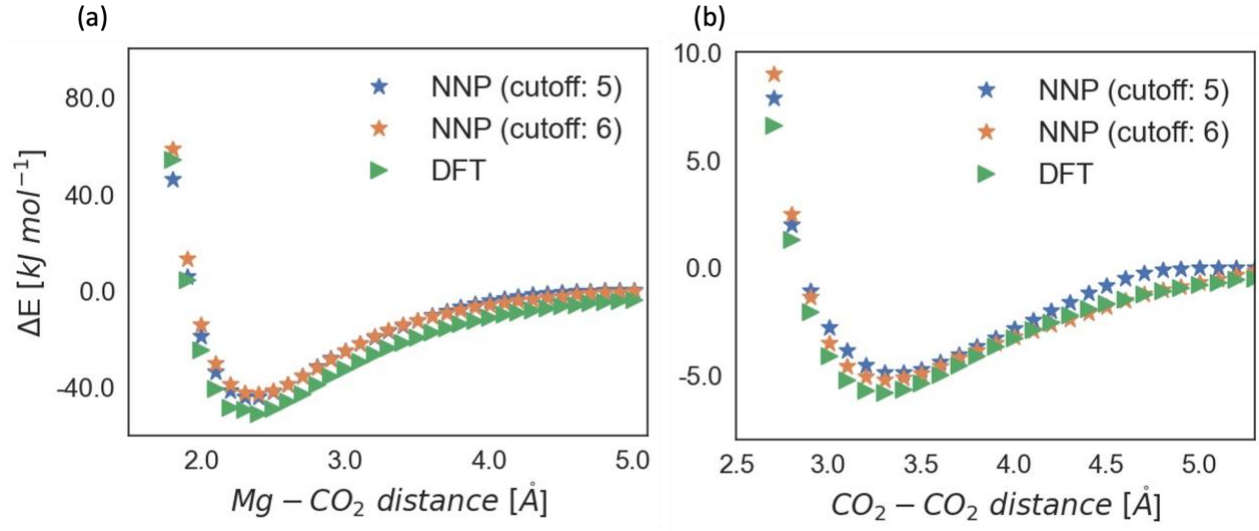


Figure 5. Comparison of NNP-predicted and DFT-calculated 1-D interaction energy profiles for (a) Mg–CO_2 and b) CO_2–CO_2 interactions.

https://doi.org/10.26434/chemrxiv-2025-c85xt **ORCID:** https://orcid.org/0000-0001-7834-3132 Content not peer-reviewed by ChemRxiv. **License:** CC BY-NC-ND 4.0

Table 1. Comparison of NNP-predicted equilibrium lattice constants and total volume of Mg-MOF-74 with the experimental data [25].

Lattice Parameters (Å)	Experiment	NNP	Difference
a	25.907	25.947	0.04
b	25.907	25.9477	0.0398
c	6.917	6.933	**0.016**
Volume ($Å^3$)	4020.447	4042.577	**22.13 (0.54%)**

After validating the reliability of the NNP on both fragments and the bulk MOF structure, CO_2 adsorption simulations were initially conducted using NNP-based fixed frame (hereinafter referred to as "rigid GCMC"), where the Mg-MOF-74 framework was treated as rigid. The rigid GCMC simulations were first performed at 298 K in the pressure range of 0-1 bar where classical force fields typically fail to accurately predict experimental data, and the simulation results were compared with experimental data [62] in **Figure S4**. The NNP-based rigid GCMC results were found to be in good agreement with the experimental values, indicating that the classical force fields' inability to capture strong guest–MOF interactions has been significantly mitigated by employing our NNP-based force fields. As a result, interactions within the guest–MOF system were described more accurately, leading to gas adsorption predictions that align closely with experimental observations. Additionally, adsorption isotherms were obtained using NNP-based rigid GCMC simulations over a temperature range of 323-463 K at 0.1-1 bar. **Figure S5** shows that at higher temperatures, the adsorption values predicted by NNP-based rigid GCMC simulations begin to diverge from the experimental data.

In rigid GCMC simulations, the performance of the NNP was significantly better than that of classical force fields (**Figure S4**). However, while accurate predictions were achieved at 298 K and within the 0-0.1 bar low pressure range, notable deviations from experimental values were observed at higher pressure (0.1-10 bar). We attributed this disagreement to the rigid treatment of the MOF structure and subsequently performed GCMC simulations with a flexible MOF framework (hereinafter referred to as "flexible GCMC") using the protocol described above. The

https://doi.org/10.26434/chemrxiv-2025-c85xt **ORCID:** https://orcid.org/0000-0001-7834-3132 Content not peer-reviewed by ChemRxiv. **License:** CC BY-NC-ND 4.0

results of flexible GCMC simulations performed at 298 K in the pressure range of 0.1-20 bar were in a better agreement with experimental values compared to rigid GCMC simulations as shown in **Figure 6**, specifically between 0.1 and 1 bar, where structural flexibility has a significant effect on the gas adsorption behavior.

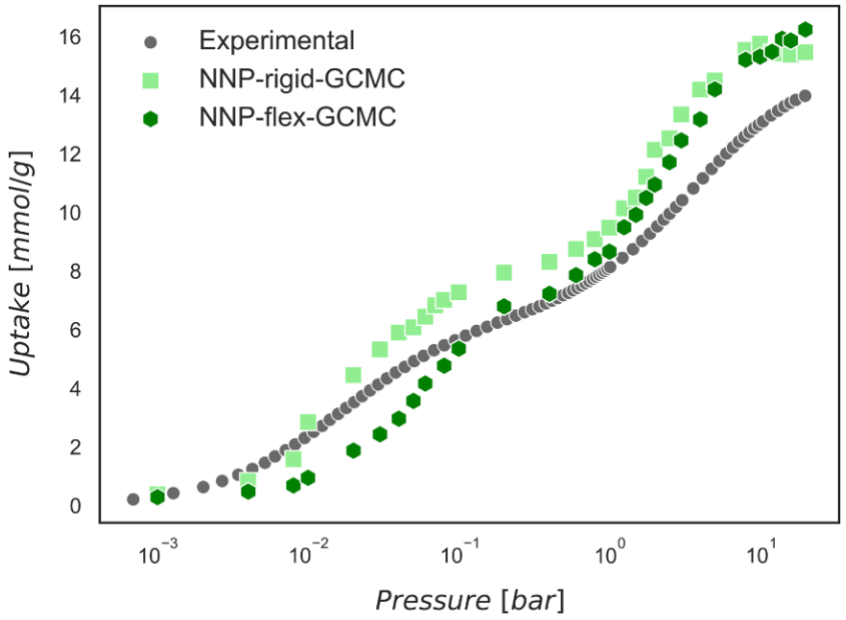


Figure 6. CO_2 adsorption isotherm obtained from NNP-based hybrid MD/GCMC simulations, compared with rigid GCMC simulations and experimental data [62] at 298 K to 20 bar.

To obtain deeper insights into the differences between rigid and flexible GCMC adsorption mechanisms, we analyzed the probability distribution of CO_2 at 0.1 bar for both rigid and flexible frameworks. In **Figure 7,** darker regions indicate low probabilities, while lighter regions represent high probabilities of finding CO_2 molecules. At 0.1 bar, where flexible GCMC outperforms rigid GCMC in terms of agreement with experimental results, both simulation methods show that CO_2 molecules primarily accumulate around the Mg open metal sites (Mg-OMS), which are the most energetically favorable adsorption sites. However, as shown in **Figure 7(a)** for the rigid framework, CO_2 molecules are more localized, whereas in the flexible framework (**Figure 7(b)**) they exhibit a more delocalized and homogeneous distribution. These findings suggest that in the low-pressure regime (0.1-1.0 bar), where CO_2–MOF interactions dominate, framework flexibility plays a crucial role in modifying adsorption sites and enhancing agreement with experimental data. In this regard, the flexibility of the MOF structure captured through NNP-based flexible GCMC

https://doi.org/10.26434/chemrxiv-2025-c85xt **ORCID:** https://orcid.org/0000-0001-7834-3132 Content not peer-reviewed by ChemRxiv. **License:** CC BY-NC-ND 4.0

simulations enables a more realistic representation of the adsorption mechanism by more accurately accommodating the guest molecules. At 10 bar (**Figure S6**), where rigid and flexible GCMC simulations predict similar adsorption values, the adsorption sites become fully occupied, leaving little room for structural adjustments. Consequently, CO_2 molecules are distributed similarly in both rigid and flexible GCMC simulations, indicating that at high loadings, framework flexibility has a diminished effect on adsorption behavior.

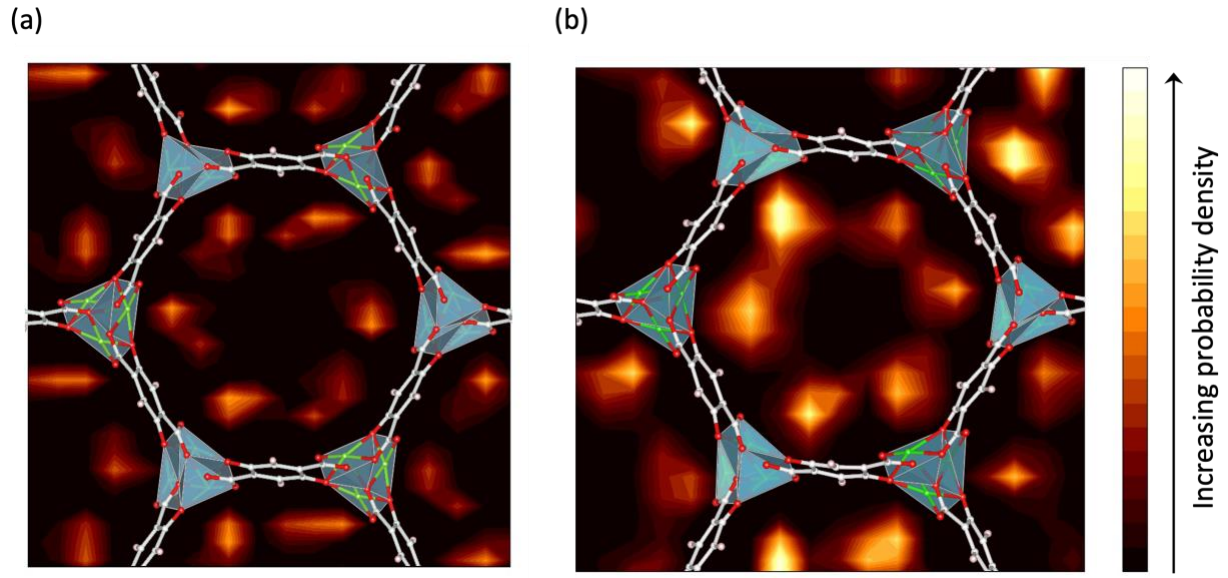


Figure 7. Calculated probability distribution of CO_2 in Mg-MOF-74 obtained from (a) rigid, (b) flexible GCMC simulations at 0.1 bar and 298 K.

The radial distribution function (RDF) was calculated for the Mg–CO_2 pair to better understand the interactions between the CO_2 molecules and the metal centers of the MOF. In **Figure 8**, the first peak in the RDF corresponds to the most probable distance between Mg atoms and CO_2 molecules, indicating preferential adsorption sites. To further explore the influence of framework flexibility, RDFs were compared between rigid and flexible GCMC simulations. Notably, in the flexible framework–as seen in the **Figure 8(a)**–the second RDF peak was sharper and slightly shifted toward shorter distances, suggesting stronger interactions due to the structural relaxation of the MOF around the adsorbed CO_2. However, at higher pressure (**Figure 8(b)**), the RDFs from flexible and rigid simulations were quite similar. This convergence can be attributed to the saturation of adsorption sites at high loading, where the availability of accessible Mg sites becomes the dominant factor, and structural flexibility plays a reduced role. In these higher

https://doi.org/10.26434/chemrxiv-2025-c85xt **ORCID:** https://orcid.org/0000-0001-7834-3132 Content not peer-reviewed by ChemRxiv. **License:** CC BY-NC-ND 4.0

pressures, most adsorption site occurs in already occupied, minimizing the impact of framework flexibility on the spatial distribution of CO_2 molecules.

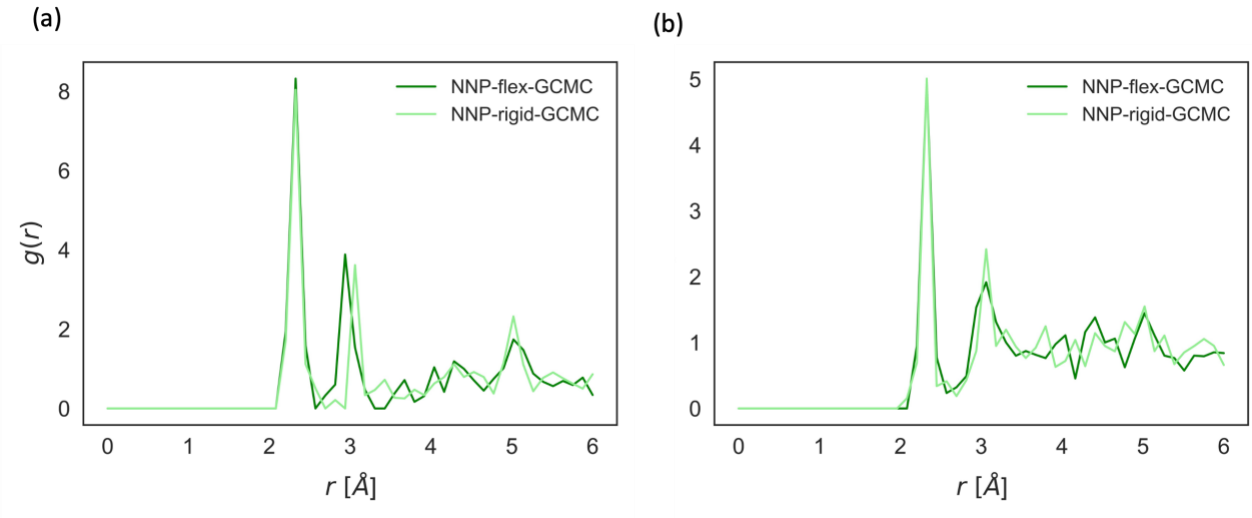


Figure 8. Calculated RDFs for the Mg–CO_2 pair at (a) 0.1 bar (b) 10 bar.

To further explore the impact of framework flexibility across different temperature conditions, flexible GCMC simulations were performed over a temperature range of 278-450 K at two representative pressures (0.1 and 1 bar). **Figure 9(a)** shows that at 0.1 bar, the flexible GCMC simulations showed excellent agreement with experimental adsorption data, while the rigid simulations significantly deviated from the experimental isotherms, especially at higher temperatures. This can be attributed to the fact that under low-pressure and higher temperature conditions, adsorption primarily occurs at high-affinity adsorption sites, such as open metal centers. This clarification is further supported by the similar deviations observed between rigid and flexible GCMC predictions from experimental values at relatively higher pressures, as shown in **Figure 9(b)**. In the rigid framework, atomic positions remain fixed, preventing structural adjustments that could enhance CO_2 binding. As a result, the rigid framework underestimates adsorption due to its inability to fully optimize host–guest interactions. In contrast, the flexible framework accommodates structural relaxation, allowing the MOF to slightly adjust its atomic positions in response to CO_2 molecules. This flexibility improves the energy landscape for adsorption, leading to higher accuracy in predicting experimental trends.

https://doi.org/10.26434/chemrxiv-2025-c85xt **ORCID:** https://orcid.org/0000-0001-7834-3132 Content not peer-reviewed by ChemRxiv. **License:** CC BY-NC-ND 4.0

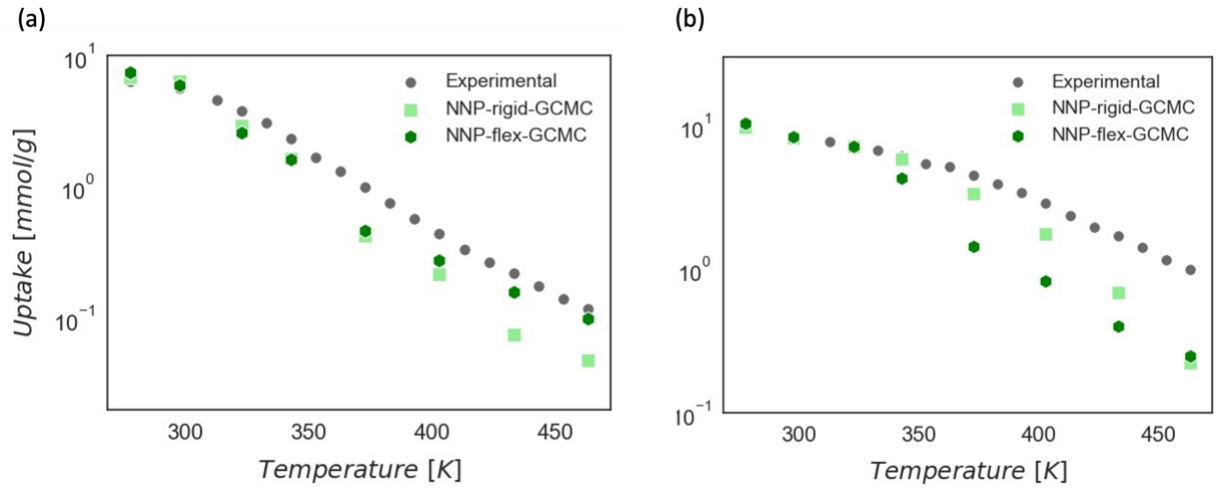


Figure 9. Adsorption isobars obtained from NNP-based hybrid MD/GCMC simulations compared with the results obtained from the rigid GCMC simulations and experimental data at (a) 0.1 bar, (b) 1 bar between the temperatures of 278-463 K.

4. Conclusion:

In this work, we developed a neural network potential (NNP) trained on DFT data derived from a single representative fragment of the Mg-MOF-74 framework with CO_2 molecules. Despite the limited training domain, the NNP accurately captured both intra- and intermolecular interactions in the CO_2–Mg-MOF-74 system, including those involving OMS. Notably, the fragment-trained model predicts the lattice parameters of the full periodic structure with excellent accuracy (0.54% deviation), demonstrating its strong transferability. We integrated this NNP into both rigid and flexible GCMC simulations to study CO_2 adsorption. The NNP- based rigid GCMC simulations showed significantly better agreement with the experimental results compared to their classical force fields counterparts, particularly in the low-pressure regime at 298 K. However, deviations at higher pressures revealed the limitations of a rigid framework treatment. By incorporating framework flexibility through a hybrid NNP-based MD/GCMC workflow, we achieved significantly improved agreement with the experimentally reported adsorption isotherm across a broader pressure range. Further analysis of CO_2 distributions revealed that flexibility enhances the delocalization and accessibility of adsorption sites at low pressures (0.1-1 bar), leading to a more realistic depiction of the host–guest interactions. These observations underscore the critical role of framework dynamics in shaping the adsorption mechanisms and demonstrate the value of using NNP-based flexible GCMC simulations to realistically simulate complex adsorption behavior in OMS-containing MOFs.

https://doi.org/10.26434/chemrxiv-2025-c85xt **ORCID:** https://orcid.org/0000-0001-7834-3132 Content not peer-reviewed by ChemRxiv. **License:** CC BY-NC-ND 4.0

Acknowledgements: The numerical calculations reported in this study were performed at TUBITAK ULAKBIM, High Performance and Grid Computing Center (TRUBA resources). This work was supported by Scientific and Technological Research Council of Turkey–TUBITAK BIDEB National Scholarship Program for Postdoctoral Researchers (Project Number 122C159).

Data Availability: The pre-trained NNP models, developed using the NequIP neural network architecture, along with the corresponding training dataset and a custom Python-based MD/GCMC implementation for NNP-based adsorption simulations, are available at: https://github.com/otayfuroglu/deepMDMC/tree/main.

Supplementary Information: Details of computational methods; changes in the number of adsorbed CO_2 molecules, volume, and temperature over time during flexible MD/GCMC simulations of Mg-MOF-74; training and validation loss curves; CO_2 adsorption isotherms on Mg-MOF-74 from rigid GCMC simulations under different conditions; probability distributions of CO_2 in Mg-MOF-74.

References:

[1] R.E. Morris, P.S. Wheatley, Gas storage in nanoporous materials, Angewandte Chemie - International Edition 47 (2008) 4966–4981. https://doi.org/10.1002/anie.200703934.

[2] O.K. Farha, I. Eryazici, N.C. Jeong, B.G. Hauser, C.E. Wilmer, A.A. Sarjeant, R.Q. Snurr, S.T. Nguyen, A.Ö. Yazaydin, J.T. Hupp, Metal-organic framework materials with ultrahigh surface areas: Is the sky the limit?, J Am Chem Soc 134 (2012) 15016–15021. https://doi.org/10.1021/ja3055639.

[3] D.A. Gómez-Gualdrón, P.Z. Moghadam, J.T. Hupp, O.K. Farha, R.Q. Snurr, Application of Consistency Criteria to Calculate BET Areas of Micro- and Mesoporous Metal-Organic Frameworks, J Am Chem Soc 138 (2016) 215–224. https://doi.org/10.1021/jacs.5b10266.

[4] D.A. Gómez-Gualdrón, Y.J. Colón, X. Zhang, T.C. Wang, Y.S. Chen, J.T. Hupp, T. Yildirim, O.K. Farha, J. Zhang, R.Q. Snurr, Evaluating topologically diverse metal-organic frameworks for cryo-adsorbed hydrogen storage, Energy Environ Sci 9 (2016) 3279–3289. https://doi.org/10.1039/c6ee02104b.

[5] J.A. Mason, J. Oktawiec, M.K. Taylor, M.R. Hudson, J. Rodriguez, J.E. Bachman, M.I. Gonzalez, A. Cervellino, A. Guagliardi, C.M. Brown, P.L. Llewellyn, N. Masciocchi, J.R.

https://doi.org/10.26434/chemrxiv-2025-c85xt **ORCID:** https://orcid.org/0000-0001-7834-3132 Content not peer-reviewed by ChemRxiv. **License:** CC BY-NC-ND 4.0

Long, Methane storage in flexible metal-organic frameworks with intrinsic thermal management, Nature 527 (2015) 357–361. https://doi.org/10.1038/nature15732.

[6] L. Li, Y. Wang, X. Wang, Y. Chen, J. Yang, J. Li, Selective gas adsorption and separation in flexible metal-organic frameworks, Huagong Jinzhan/Chemical Industry and Engineering Progress 35 (2016) 1794–1803. https://doi.org/10.16085/j.issn.1000-6613.2016.06.020.

[7] J.M. Holcroft, K.J. Hartlieb, P.Z. Moghadam, J.G. Bell, G. Barin, D.P. Ferris, E.D. Bloch, M.M. Algaradah, M.S. Nassar, Y.Y. Botros, K.M. Thomas, J.R. Long, R.Q. Snurr, J.F. Stoddart, Carbohydrate-mediated purification of petrochemicals, J Am Chem Soc 137 (2015) 5706–5719. https://doi.org/10.1021/ja511878b.

[8] J.B. Decoste, G.W. Peterson, Metal-organic frameworks for air purification of toxic chemicals, Chem Rev 114 (2014) 5695–5727. https://doi.org/10.1021/cr4006473.

[9] C. Altintas, S. Velioglu, S. Keskin, Reply to Comment on “database for CO 2 Separation Performances of MOFs Based on Computational Materials Screening,” ACS Appl Mater Interfaces 11 (2019) 16266–16271. https://doi.org/10.1021/acsami.9b02614.

[10] P. Horcajada, T. Chalati, C. Serre, B. Gillet, C. Sebrie, T. Baati, J.F. Eubank, D. Heurtaux, P. Clayette, C. Kreuz, J.S. Chang, Y.K. Hwang, V. Marsaud, P.N. Bories, L. Cynober, S. Gil, G. Férey, P. Couvreur, R. Gref, Porous metal-organic-framework nanoscale carriers as a potential platform for drug deliveryand imaging, Nat Mater 9 (2010) 172–178. https://doi.org/10.1038/nmat2608.

[11] P. Li, J.A. Modica, A.J. Howarth, E. Vargas L., P.Z. Moghadam, R.Q. Snurr, M. Mrksich, J.T. Hupp, O.K. Farha, Toward Design Rules for Enzyme Immobilization in Hierarchical Mesoporous Metal-Organic Frameworks, Chem 1 (2016) 154–169. https://doi.org/10.1016/j.chempr.2016.05.001.

[12] T. Faust, Nanomedicine: MOFs deliver, Nat Chem 7 (2015) 270–271. http://www.nature.com/doifinder/10.1038/nchem.2229.

[13] M.C. Bernini, D. Fairen-Jimenez, M. Pasinetti, A.J. Ramirez-Pastor, R.Q. Snurr, Screening of bio-compatible metal-organic frameworks as potential drug carriers using Monte Carlo simulations, J Mater Chem B 2 (2014) 766–774. https://doi.org/10.1039/c3tb21328e.

[14] L.E. Kreno, K. Leong, O.K. Farha, M. Allendorf, R.P. Van Duyne, J.T. Hupp, No Title, Chem. Rev. 112 (2012) 1105.

https://doi.org/10.26434/chemrxiv-2025-c85xt **ORCID:** https://orcid.org/0000-0001-7834-3132 Content not peer-reviewed by ChemRxiv. **License:** CC BY-NC-ND 4.0

[15] A. Corma, From microporous to mesoporous molecular sieve materials and their use in catalysis, Chem Rev 97 (1997) 2373–2419. https://doi.org/10.1021/cr960406n.

[16] A. Corma, H. García, F.X. Llabrés I Xamena, Engineering metal organic frameworks for heterogeneous catalysis, Chem Rev 110 (2010) 4606–4655. https://doi.org/10.1021/cr9003924.

[17] Ü. Kökçam-Demir, A. Goldman, L. Esrafili, M. Gharib, A. Morsali, O. Weingart, C. Janiak, Coordinatively unsaturated metal sites (open metal sites) in metal-organic frameworks: Design and applications, Chem Soc Rev 49 (2020). https://doi.org/10.1039/c9cs00609e.

[18] J. Ha, M. Jung, J. Park, H. Oh, H.R. Moon, Thermodynamic Separation of Hydrogen Isotopes Using Hofmann-Type Metal-Organic Frameworks with High-Density Open Metal Sites, ACS Appl Mater Interfaces 14 (2022). https://doi.org/10.1021/acsami.2c07829.

[19] B. Chen, N.W. Ockwig, A.R. Millward, D.S. Contreras, O.M. Yaghi, High H2 adsorption in a microporous metal-organic framework with open metal sites, Angewandte Chemie - International Edition 44 (2005). https://doi.org/10.1002/anie.200462787.

[20] P.D.C. Dietzel, R. Blom, H. Fjellvåg, Base-induced formation of two magnesium metal-organic framework compounds with a bifunctional tetratopic ligand, Eur J Inorg Chem (2008). https://doi.org/10.1002/ejic.200701284.

[21] D. Britt, H. Furukawa, B. Wang, T.G. Glover, O.M. Yaghi, Highly efficient separation of carbon dioxide by a metal-organic framework replete with open metal sites, Proc Natl Acad Sci U S A 106 (2009) 20637–20640. https://doi.org/10.1073/pnas.0909718106.

[22] W.L. Queen, M.R. Hudson, E.D. Bloch, J.A. Mason, M.I. Gonzalez, J.S. Lee, D. Gygi, J.D. Howe, K. Lee, T.A. Darwish, M. James, V.K. Peterson, S.J. Teat, B. Smit, J.B. Neaton, J.R. Long, C.M. Brown, Comprehensive study of carbon dioxide adsorption in the metal-organic frameworks M2(dobdc) (M = Mg, Mn, Fe, Co, Ni, Cu, Zn), Chem Sci 5 (2014). https://doi.org/10.1039/c4sc02064b.

[23] Z.R. Herm, R. Krishna, J.R. Long, CO 2/CH 4, CH 4/H 2 and CO 2/CH 4/H 2 separations at high pressures using Mg 2(dobdc), Microporous and Mesoporous Materials 151 (2012). https://doi.org/10.1016/j.micromeso.2011.09.004.

[24] P.D.C. Dietzel, V. Besikiotis, R. Blom, Application of metal-organic frameworks with coordinatively unsaturated metal sites in storage and separation of methane and carbon dioxide, J Mater Chem 19 (2009). https://doi.org/10.1039/b911242a.

https://doi.org/10.26434/chemrxiv-2025-c85xt **ORCID:** https://orcid.org/0000-0001-7834-3132 Content not peer-reviewed by ChemRxiv. **License:** CC BY-NC-ND 4.0

[25] B. Pato-Doldán, M.H. Rosnes, P.D.C. Dietzel, An In-Depth Structural Study of the Carbon Dioxide Adsorption Process in the Porous Metal–Organic Frameworks CPO-27-M, ChemSusChem 10 (2017). https://doi.org/10.1002/cssc.201601752.

[26] Z. Bao, L. Yu, Q. Ren, X. Lu, S. Deng, Adsorption of CO2 and CH4 on a magnesium-based metal organic framework, J Colloid Interface Sci 353 (2011). https://doi.org/10.1016/j.jcis.2010.09.065.

[27] L. Valenzano, B. Civalleri, S. Chavan, G.T. Palomino, C.O. Areán, S. Bordiga, Computational and experimental studies on the adsorption of CO, N 2, and CO2 on Mg-MOF-74, Journal of Physical Chemistry C 114 (2010) 11185–11191. https://doi.org/10.1021/jp102574f.

[28] S. Xiang, W. Zhou, Z. Zhang, M.A. Green, Y. Liu, B. Chen, Open Metal Sites within Isostructural Metal–Organic Frameworks for Differential Recognition of Acetylene and Extraordinarily High Acetylene Storage Capacity at Room Temperature, Angewandte Chemie 122 (2010). https://doi.org/10.1002/ange.201000094.

[29] R. Goeminne, V. Van Speybroeck, Ab Initio Predictions of Adsorption in Flexible Metal–Organic Frameworks for Water Harvesting Applications, J Am Chem Soc 147 (2025) 3615–3630. https://doi.org/10.1021/jacs.4c15287.

[30] L.C. Lin, K. Lee, L. Gagliardi, J.B. Neaton, B. Smit, Force-field development from electronic structure calculations with periodic boundary conditions: Applications to gaseous adsorption and transport in metal-organic frameworks, J Chem Theory Comput 10 (2014). https://doi.org/10.1021/ct500094w.

[31] R. Mercado, B. Vlaisavljevich, L.C. Lin, K. Lee, Y. Lee, J.A. Mason, D.J. Xiao, M.I. Gonzalez, M.T. Kapelewski, J.B. Neaton, B. Smit, Force Field Development from Periodic Density Functional Theory Calculations for Gas Separation Applications Using Metal-Organic Frameworks, Journal of Physical Chemistry C 120 (2016) 12590–12604. https://doi.org/10.1021/acs.jpcc.6b03393.

[32] C. Campbell, J.R.B. Gomes, M. Fischer, M. Jorge, New Model for Predicting Adsorption of Polar Molecules in Metal-Organic Frameworks with Unsaturated Metal Sites, Journal of Physical Chemistry Letters 9 (2018). https://doi.org/10.1021/acs.jpclett.8b00967.

[33] M. V. Parkes, H. Demir, S.L. Teich-Mcgoldrick, D.S. Sholl, J.A. Greathouse, M.D. Allendorf, Molecular dynamics simulation of framework flexibility effects on noble gas

https://doi.org/10.26434/chemrxiv-2025-c85xt **ORCID:** https://orcid.org/0000-0001-7834-3132 Content not peer-reviewed by ChemRxiv. **License:** CC BY-NC-ND 4.0

diffusion in HKUST-1 and ZIF-8, Microporous and Mesoporous Materials 194 (2014). https://doi.org/10.1016/j.micromeso.2014.03.027.

[34] S.L. Mayo, B.D. Olafson, W.A. Goddard, DREIDING: A generic force field for molecular simulations, Journal of Physical Chemistry 94 (1990). https://doi.org/10.1021/j100389a010.

[35] M.A. Addicoat, N. Vankova, I.F. Akter, T. Heine, Extension of the universal force field to metal-organic frameworks, J Chem Theory Comput 10 (2014). https://doi.org/10.1021/ct400952t.

[36] M.G. Martin, J.I. Siepmann, Transferable potentials for phase equilibria. 1. United-atom description of n-alkanes, Journal of Physical Chemistry B 102 (1998) 2569–2577. https://doi.org/10.1021/jp972543+.

[37] Z. Li, K. Shi, D. Dubbeldam, M. Dewing, C. Knight, Á. Vázquez-Mayagoitia, R.Q. Snurr, Efficient Implementation of Monte Carlo Algorithms on Graphical Processing Units for Simulation of Adsorption in Porous Materials, J Chem Theory Comput 20 (2024) 10649–10666. https://doi.org/10.1021/acs.jctc.4c01058.

[38] L. Chen, L. Grajciar, P. Nachtigall, T. Düren, Accurate prediction of methane adsorption in a metal-organic framework with unsaturated metal sites by direct implementation of an ab initio derived potential energy surface in GCMC simulation, Journal of Physical Chemistry C 115 (2011). https://doi.org/10.1021/jp2090878.

[39] A. Kundu, G. Piccini, K. Sillar, J. Sauer, Ab Initio Prediction of Adsorption Isotherms for Small Molecules in Metal-Organic Frameworks, J Am Chem Soc 138 (2016) 14047–14056. https://doi.org/10.1021/jacs.6b08646.

[40] A. Kundu, K. Sillar, J. Sauer, Ab Initio Prediction of Adsorption Isotherms for Gas Mixtures by Grand Canonical Monte Carlo Simulations on a Lattice of Sites, Journal of Physical Chemistry Letters 8 (2017). https://doi.org/10.1021/acs.jpclett.7b01205.

[41] E.O. Fetisov, M.S. Shah, J.R. Long, M. Tsapatsis, J. Ilja Siepmann, First principles Monte Carlo simulations of unary and binary adsorption: CO2, N2, and H2O in Mg-MOF-74, Chemical Communications 54 (2018). https://doi.org/10.1039/c8cc06178e.

[42] M. Dixit, T.A. Maark, S. Pal, Ab initio and periodic DFT investigation of hydrogen storage on light metal-decorated MOF-5, Int J Hydrogen Energy 36 (2011). https://doi.org/10.1016/j.ijhydene.2011.05.165.

https://doi.org/10.26434/chemrxiv-2025-c85xt **ORCID:** https://orcid.org/0000-0001-7834-3132 Content not peer-reviewed by ChemRxiv. **License:** CC BY-NC-ND 4.0

[43] A. Samanta, T. Furuta, J. Li, Theoretical assessment of the elastic constants and hydrogen storage capacity of some metal-organic framework materials, Journal of Chemical Physics 125 (2006). https://doi.org/10.1063/1.2337287.

[44] D. Antypov, A. Shkurenko, P.M. Bhatt, Y. Belmabkhout, K. Adil, A. Cadiau, M. Suyetin, M. Eddaoudi, M.J. Rosseinsky, M.S. Dyer, Differential guest location by host dynamics enhances propylene/propane separation in a metal-organic framework, Nat Commun 11 (2020). https://doi.org/10.1038/s41467-020-19207-9.

[45] M. Eckhoff, J. Behler, From Molecular Fragments to the Bulk: Development of a Neural Network Potential for MOF-5, J Chem Theory Comput 15 (2019) 3793–3809. https://doi.org/10.1021/acs.jctc.8b01288.

[46] O. Tayfuroglu, A. Kocak, Y. Zorlu, A neural network potential for the IRMOF series and its application for thermal and mechanical behaviors †, Phys. Chem. Chem. Phys 24 (2022) 11882–11897. https://doi.org/10.1039/d1cp05973d.

[47] R. Goeminne, L. Vanduyfhuys, V. Van Speybroeck, T. Verstraelen, DFT-Quality Adsorption Simulations in Metal-Organic Frameworks Enabled by Machine Learning Potentials, J Chem Theory Comput 19 (2023). https://doi.org/10.1021/acs.jctc.3c00495.

[48] S. Mandal, P.K. Maiti, Prediction of thermal conductivity in CALF-20 with first-principles accuracy via machine learning interatomic potentials, Commun Mater 6 (2025) 22. https://doi.org/10.1038/s43246-025-00745-y.

[49] S. Wieser, E. Zojer, Machine learned force-fields for an Ab-initio quality description of metal-organic frameworks, NPJ Comput Mater 10 (2024). https://doi.org/10.1038/s41524-024-01205-w.

[50] A. Sharma, S. Sanvito, Quantum-accurate machine learning potentials for metal-organic frameworks using temperature driven active learning, NPJ Comput Mater 10 (2024) 237. https://doi.org/10.1038/s41524-024-01427-y.

[51] N. Castel, D. André, C. Edwards, J.D. Evans, F.-X. Coudert, Machine learning interatomic potentials for amorphous zeolitic imidazolate frameworks, Digital Discovery 3 (2024) 355–368. https://doi.org/10.1039/D3DD00236E.

[52] B. Mehlig, D.W. Heermann, B.M. Forrest, Hybrid Monte Carlo method for condensed-matter systems, Phys Rev B 45 (1992) 679–685. https://doi.org/10.1103/PhysRevB.45.679.

https://doi.org/10.26434/chemrxiv-2025-c85xt **ORCID:** https://orcid.org/0000-0001-7834-3132 Content not peer-reviewed by ChemRxiv. **License:** CC BY-NC-ND 4.0

[53] J. Guo, A. Haji-Akbari, J.C. Palmer, Hybrid Monte Carlo with LAMMPS, J Theor Comput Chem 17 (2018) 1840002. https://doi.org/10.1142/S0219633618400023.

[54] N. Chanut, A. Ghoufi, M.-V. Coulet, S. Bourrelly, B. Kuchta, G. Maurin, P.L. Llewellyn, Tailoring the separation properties of flexible metal-organic frameworks using mechanical pressure, Nat Commun 11 (2020) 1216. https://doi.org/10.1038/s41467-020-15036-y.

[55] Z. Yu, D.M. Anstine, S.E. Boulfelfel, C. Gu, C.M. Colina, D.S. Sholl, Incorporating Flexibility Effects into Metal–Organic Framework Adsorption Simulations Using Different Models, ACS Appl Mater Interfaces 13 (2021) 61305–61315. https://doi.org/10.1021/acsami.1c20583.

[56] S.K. Achar, J.J. Wardzala, L. Bernasconi, L. Zhang, J.K. Johnson, Combined Deep Learning and Classical Potential Approach for Modeling Diffusion in UiO-66, J Chem Theory Comput 18 (2022) 3593–3606. https://doi.org/10.1021/acs.jctc.2c00010.

[57] O. Tayfuroglu, A. Kocak, Y. Zorlu, Modeling Gas Adsorption and Mechanistic Insights into Flexibility in Isoreticular Metal–Organic Frameworks Using High-Dimensional Neural Network Potentials, Langmuir 41 (2025) 7323–7335. https://doi.org/10.1021/acs.langmuir.4c04578.

[58] B. Zheng, G.X. Gu, C. dos Santos, R. Neumann Barros Ferreira, M. Steiner, B. Luan, Simulating CO2 diffusivity in rigid and flexible Mg-MOF-74 with machine-learning force fields, APL Machine Learning 2 (2024). https://doi.org/10.1063/5.0190372.

[59] S. Batzner, A. Musaelian, L. Sun, M. Geiger, J.P. Mailoa, M. Kornbluth, N. Molinari, T.E. Smidt, B. Kozinsky, E(3)-equivariant graph neural networks for data-efficient and accurate interatomic potentials, Nat Commun 13 (2022) 2453. https://doi.org/10.1038/s41467-022-29939-5.

[60] S. Vandenhaute, M. Cools-Ceuppens, S. DeKeyser, T. Verstraelen, V. Van Speybroeck, Machine learning potentials for metal-organic frameworks using an incremental learning approach, NPJ Comput Mater 9 (2023). https://doi.org/10.1038/s41524-023-00969-x.

[61] Y.G. Chung, E. Haldoupis, B.J. Bucior, M. Haranczyk, S. Lee, H. Zhang, K.D. Vogiatzis, M. Milisavljevic, S. Ling, J.S. Camp, B. Slater, J.I. Siepmann, D.S. Sholl, R.Q. Snurr, Advances, Updates, and Analytics for the Computation-Ready, Experimental Metal–Organic Framework Database: CoRE MOF 2019, J Chem Eng Data 64 (2019) 5985–5998. https://doi.org/10.1021/acs.jced.9b00835.

https://doi.org/10.26434/chemrxiv-2025-c85xt **ORCID:** https://orcid.org/0000-0001-7834-3132 Content not peer-reviewed by ChemRxiv. **License:** CC BY-NC-ND 4.0

[62] D. Yu, A.O. Yazaydin, J.R. Lane, P.D.C. Dietzel, R.Q. Snurr, A combined experimental and quantum chemical study of CO2 adsorption in the metal-organic framework CPO-27 with different metals, Chem Sci 4 (2013). https://doi.org/10.1039/c3sc51319j.

https://doi.org/10.26434/chemrxiv-2025-c85xt **ORCID:** https://orcid.org/0000-0001-7834-3132 Content not peer-reviewed by ChemRxiv. **License:** CC BY-NC-ND 4.0